RSC Advances

ROYAL SOCIETY OF CHEMISTRY

www.rsc.org/advances

A novel Fe_3O_4/CdTe fluorescence probe for sialic acid detection based on phenylboronic acid- sialic acid recognition system

Jinna Wang, Guanhong Xu, Fangdi Wei, Jing Yang, Ping Zhou, Qin Hu*

School of Pharmacy, Nanjing Medical University, Nanjing, Jiangsu 211166, PR China

Abstract

A novel fluorescence method was established for detecting sialic acid (SA) by using phenylboronic acid (PBA)-functionalized Fe_3O_4/CdTe magnetic nanoparticles as fluorescence probe. Initially, Fe_3O_4 nanoparticles were modified with amino groups, and then 3-mercapto propionic acid-stabilized CdTe quantum dots (QDs) were covalently linked to the amino-modified Fe_3O_4 nanoparticles to form Fe_3O_4/CdTe magnetic fluorescence nanoparticles. Finally, PBA was introduced on the surface of Fe_3O_4/CdTe to form PBA-functionalized Fe_3O_4/CdTe magnetic fluorescence nanoparticles. This kind of nanoparticles can specifically recognize SA and its fluorescence intensity is quenched by SA. In addition, the conjugate of the nanoparticles and SA is easy to separate from the sample matrix due to its magnetism. Therefore, this nanoparticle can be used as a fluorescence probe to detect SA. Under the optimal conditions, the fluorescence intensity of the nano probe was found to be inversely linear with the concentration of SA in a wide range of 50 μg/ml-1.50 mg/ml, and the limit of detection was 16 μg/ml. PBA-functionalized Fe_3O_4/CdTe nano probe was applied to the determination of SA in infant formula, and the result showed high accuracy and precision. PBA-functionalized Fe_3O_4/CdTe nano probe has a potential to be used to monitor SA in food.

1. Introduction

Sialic acid (SA) is a kind of 9-carbon monosaccharide derivatives, frequently found at the terminal position of glycoconjugates.[1] There are animal models confirming that insufficiency of SA intake influences mental development and learning ability.[2] Since SA plays an important role in brain growth, some famous food companies have recently launched the "SA plan",[3] which is to increase the content of SA in infant formula. However, excessive SA intake leads to occurrence of inflammation in body.[4] So, it is very important to monitor the quantity of SA added in infant formula. Some methods including colorimetry, chromatography, fluorescence and enzymatic assays are powerful for SA detection,[5-8] but these techniques have their own defects. Chromatography has high sensitivity and specificity, but it needs expensive instrument and professional operation. Although enzymatic assay of SA has shown great promise, it is limited by either expensive enzymatic reagents or time-consuming. Substance interference in complex samples is the limitation of the colorimetry and fluorescence assays. So, there is a practical need to develop new approaches for determination of SA to overcome the shortcomings of the present strategies.

Recently, quantum dots (QDs) as fluorescence probes have attracted increasing interest in determination of saccharides due to their unique optic characteristics.[9-11] Some reports have suggested that phenylboronic acid (PBA) has special binding affinity with SA in physiological environment of 7.4 compared to other saccharide.[12-16] Matsumoto et al.[17] used a gold electrode modified with PBA to detect SA at cell membranes in a potentionmetric method. Han et al.[14, 15] reported that PBA-functionalized QDs could specifically recognize and locate SA on the surface of cells, and cell imaging could be realized by this way. However, up to date, quantitative analysis of SA by PBA-functionalized QDs has not been reported.

Herein, PBA-functionalized Fe_3O_4/CdTe magnetic fluorescence nano probe was designed and prepared. PBA-functionalized Fe_3O_4/CdTe nanoparticles combined SA specifically, and the fluorescence of PBA-functionalized Fe_3O_4/CdTe nanoparticles was lineally quenched by SA. The conjugate could be easily separated from the matrix of samples due to their magnetism. An efficient and specific method to detect SA using PBA-functionalized Fe_3O_4/CdTe nanoparticles as nano probe was built, validated, and finally applied to the determination of SA in infant formula with satisfactory results.

2. Experimental section

2.1 Materials

* Corresponding author: Tel. / fax: +86-2586868468; E-mail: huqin@njmu.edu.cn

Tellurium powder (purity > 99%), sodium borohydride, 3-mercapto propionic acid (MPA), sodium hydroxide, ferric chloride hexahydrate ($FeCl_3 \cdot 6H_2O$), ferrous chloride tetrahydrate ($FeCl_2 \cdot 4H_2O$), ammonia water ($NH_3 \cdot H_2O$ 25-28%), PEG400, tetraethylorthosilicate (TEOS), $(CH_3COO)_2Cd \cdot 2H_2O$, PEG400, glucose (Glu), galactose (Gal), mannose (Man) and fructose (Fru) were purchased from Wanqing chemical industry (Nanjing, China). 3-Aminopropyl triethoxysilane (APTES), 1-(3-Dimethylaminopropyl)-3-ethylcarbodiimide hydrochloride (EDC), SA, 3-amino phenylboronic acid (PBA), and dopamine (DA) were purchased from Aladdin industrial corporation (Shanghai, China). Phosphate-buffered saline (PBS, 5mM, pH 7.4) contained 0.1M NaCl. The purified water used in the study was prepared using Direct-Q water purification system (Millipore, USA). All chemical reagents and solvents were analytical grade and used without further purification.

2.2 Instruments

FT-IR spectra were recorded by using a Tensor-27 FT-IR spectrometer (Bruker, Germany). The fluorescence emission spectra were measured on F4600 spectrofluorometer (Hitachi, Japan) with 370 nm excitation. UV-vis absorption spectra were obtained on a UV-2450 UV-Visible spectrophotometer (Hitachi, Japan). Transmission electron microscopy (TEM) images of the samples were collected on a JEM-1010 transmission electron microscope (Hitachi, Japan). The particle size was determined by dynamic light scattering (DLS)detector (Zs90, Malvern, U. K.). PBA combined on the surface of Fe_3O_4/CdTe nanoparticles was confirmed by gel electrophoresis (Shanghai Tanon HE-120) in 0.5% agarose gel with 0.5×TBE buffer (pH 8.0) at 80 v for 30 min.

2.3 Preparation of amino-modified Fe_3O_4 magnetic nanoparticles

Fe_3O_4 magnetic nanoparticles were prepared through a classic chemical co-precipitation method.[18, 19] In order to modify amino groups on Fe_3O_4 magnetic nanoparticles, hydroxyl groups were introduced firstly. PEG400 was added dropwise slowly to Fe_3O_4 suspension at 80 ^oC under mechanical stirring and N_2 protection. After 60 min, the obtained hydroxyl-modified Fe_3O_4 precipitations were magnetically separated, and washed with purified water and ethanol several times until the pH value reached 7.0. Finally, the hydroxyl-modified Fe_3O_4 precipitations were re-dispersed in 50 ml of ethanol and stored at 4 ^oC.

The amino-modified Fe_3O_4 magnetic nanoparticles were obtained by adding TEOS and APTES to the above hydroxyl-modified Fe_3O_4 precipitations solution.[20] The preparation was described in detail as follows. A suspension of hydroxyl-modified Fe_3O_4 nanoparticles (100 mg) was diluted by a mixture of purified water (20 ml) and ethanol (150 ml), and ultrasonicated for 15 min. Then, 1ml of $NH_3 \cdot H_2O$ (25 wt %) was added. After mechanical stirring at 30 ^oC for 30 min, 1 ml of TEOS was dropped slowly into the reaction solution. The reaction was continued for 45 min, and then 70 μl of APTES was added to the reaction solution. Finally, the mixture solution was mechanically stirred for another 4 h. The obtained amino-modified Fe_3O_4 magnetic nanoparticles were magnetically separated, washed with purified water and ethanol several times, and finally dried at 30 ^oC for 4 h.

2.4 Preparation of MPA-caped CdTe QDs

CdTe QDs was synthesized through the reaction between Cd^{2+} and NaHTe solution in a typical synthesis,[21] using MPA as a stabilizing agent.

2.5 Fabrication of Fe_3O_4/CdTe magnetic fluorescence nanoparticles and PBA-immobilization

The MPA-capped CdTe QDs were conjugated with amino-modified Fe_3O_4 nanoparticles through bonding carboxyl groups on QDs with amino groups on Fe_3O_4 nanoparticles.[22] The prepared CdTe QDs were concentrated 10 times, then precipitated in anhydrous ethanol, dissolved again in purified water, and adjusted pH to 7.5. In order to active the CdTe QDs, 25 mg of EDC was added to 1ml of above CdTe solution, and the mixture was ultrasonicated for 15 min. Then, 1 mg of amino-modified Fe_3O_4 was put into the mixture, and the mixture was ultrasonicated for 5 min, following by vibrating for 4 h at 25 ^oC. In order to immobilize PBA on the surface of Fe_3O_4/CdTe nanocomposites, 3mg of PBA was added into the above solution. The mixed solution was vibrated for 1 h at 25 ^oC. Finally, the obtained PBA-functionalized Fe_3O_4/CdTe magnetic fluorescence nanoparticles were washed thoroughly with PBS (pH 7.4) buffer to remove the excessive CdTe , and stored at 4 ^oC.

2.6 Fluorescence measurement

0.1 ml of the as-prepared PBA-functionalized Fe_3O_4/CdTe nanoparticles and 0.05 ml of a solution containing SA were added into a centrifuge tube containing 1 ml of PBS (5mM, pH7.4) buffer solution. The mixture was incubated at 37 ^oC for 3 h. Then, the conjugate of PBA-functionalized Fe_3O_4/CdTe nanoparticles and SA was separated by a magnet, washed out with PBS buffer. Finally, the conjugate was dispersed in 1 ml of PBS and its fluorescence intensity was recorded.

2.7 Determination of SA in infant formula

0.3 g of infant formula was dispersed in 20 ml of 0.1M H_2SO_4, centrifuged at 11000 rpm at 4 ^oC for 20 min. The upper cream layer was removed, and the rest was vortexed, and incubated at 80 ^oC for 2 h. Then, the mixture was cooled with flowing water and centrifuged at 11000 rpm at 4 ^oC for 20 min. The supernatant was evaporated, and the residual was dissolved in PBS buffer, and its pH was adjusted to 7.4 with 6 M NaOH. Finally, the volume was set to 4 ml with PBS buffer solution. The fluorescence measurement of the sample was carried out according to section 2.6.

Results and discussion

3.1 Fabrication of PBA-functionalized Fe_3O_4/CdTe nano probe and its working principle for SA detection

Scheme 1 showed the synthesis of PBA-functionalized Fe_3O_4/CdTe nano probe and its working principle for SA detection. In order to obtain Fe_3O_4/CdTe nanoparticles, amino-modified Fe_3O_4 nanoparticles were firstly prepared. Then, Fe_3O_4/CdTe magnetic fluorescence nanoparticles were obtained by binding the amino groups on Fe_3O_4 magnetic nanoparticles with the carboxyl groups on CdTe QDs. Finally, the PBA-functionalized Fe_3O_4/CdTe nano probe was successfully prepared by combining amino groups on PBA with carboxylic groups on Fe_3O_4/CdTe nanoparticles.

As shown in scheme 1., after incubating SA with the nano probe, PBA on the surface of the probe could covalently combined with *cis*-diols of SA to form five-membered cyclic complexes, which made the excited electrons from conduction band to valence band hindered.[23] So, the fluorescence intensity of the nano probe decreased with the increasing of SA, which could be attributed to the exciton energy transfer-based fluorescence responses. In addition, the thickness of the capping layer of Fe_3O_4/CdTe nanoparticles was increased and its hydrophilicity was reduced, which also made the fluorescence of the nano probe quenched.[24]

3.2 Optimization of synthesis conditions

The synthesis of PBA-functionalized Fe_3O_4/CdTe magnetic fluorescence nano probe included several steps. So its fluorescence intensity was affected by some aspects, such as the amount of APTES, EDC and PBA, concentration ratio of reactants, reaction time, pH of QDs, etc. All the influence factors were optimized.

Fig. 1a showed the fluorescence intensity of PBA-functionalized Fe_3O_4/CdTe nano probe under various ratios of QDs to Fe_3O_4. Actually, with the increase of the ratio, the fluorescence intensity of the probe increased due to more CdTe QDs anchoring on the surface of amion-modified Fe_3O_4 nanoparticles. The fluorescence intensity of the probe reached highest and kept almost no changed when the ratio was in the range of 10:1-14:1. However, when the ratio was higher than 14:1, the fluorescence intensity of PBA-functionalized Fe_3O_4/CdTe nano probe became slightly weaker due to the accumulation of QDs. Fig. 1b showed the effect of pH on the fluorescence intensity of PBA-functionalized Fe_3O_4/CdTe nano probe. It indicated that the pH value had obvious influence on the fluorescence intensity of the probe. At low pH value, the fluorescence intensity of the probe was very weak. The reason was that the sulfenly in MPA on the surface of QDs was easily protonized at low pH, which led to the drop of MPA from CdTe QDs. [25,26] It is more difficult for MPA-capped CdTe QDs to conjugate with amino-modified Fe_3O_4 nanoparticles at low pH since the conjugation was undergone through bonding carboxyl groups in MPA on QDs with amino groups on Fe_3O_4 nanoparticles. With the increase of the pH, the fluorescence intensity of the probe increased, and reached the highest value at the pH 7.5. But, when the pH was higher than 7.5, the fluorescence intensity of the probe decreased dramatically. This is because that the activity of EDC as carboxyl activating agent is low at high pH, which made the carboxyl groups on CdTe QDs not adequately activated. So, it was more difficult for MPA-capped CdTe QDs to combine with amino-modified Fe_3O_4 nanoparticles to form the nano probe at high pH. When the pH was higher than 9, the fluorescence of nano probe was slightly recovered. The reason might be that the optimal synthesis condition of CdTe QDs was at pH 9-10 and the fluorescence intensity of QDs was highest at this pH range[27], and this made the fluorescence intensity of the nano probe recovered weakly. Thus, pH value should be carefully controlled when preparing the nano probe.

The other influence factors were optimized, and the results were displayed in supplying information.

3.3 Characterization of Fe_3O_4/CdTe nanoparticles

3.3.1 Infrared spectroscopy.

FT-IR spectra of Fe_3O_4, amino-modified Fe_3O_4, Fe_3O_4/CdTe nanoparticles are shown in Fig. 2a, Fig. 2b. and Fig. 2c, respectively. The obvious peaks at 574 cm^{-1} in Fig. 2(a. b. c) corresponded to the stretching vibration of Fe-O bond. The peaks at 1067 and 465 cm^{-1} in Fig. 2(b. c) were attributed to the stretching and deformation vibrations

of SiO_2, which suggested the successful coating of silica on the surface of the magnetic nanoparticles. In addition, the peak at 1553 cm^{-1} in Fig. 2b was attributed to the bending vibrations of amino groups, which indicated that amino groups were successfully introduced onto Fe_3O_4 nanoparticles surface. The peak at 1694 cm^{-1} in Fig. 2c corresponded to the stretching vibration of carboxyl groups, reflecting the existence of carboxyl groups in Fe_3O_4/CdTe nanoparticles since MPA was used to modify QDs. These results showed that CdTe QDs were well conjugated with amino-modified Fe_3O_4 nanoparticles.

3.3.2 Transmission electron microscopy.

Fig. 3 showed TEM images of Fe_3O_4, amino-modified Fe_3O_4 and Fe_3O_4/CdTe nanoparticles. As shown in Fig. 3a, Fe_3O_4 nanoparticles were approximately spherical, and the average size was about 20 nm. After modified with amino groups, the thickness of Fe_3O_4 nanoparticles increased. The mean size of amino-modified Fe_3O_4 nanoparticles was approximately 50 nm according to Fig. 3b. As is well seen, Fig. 3c showed the representative TEM image of Fe_3O_4/CdTe nanoparticles and the average diameter of the nanoparticles was about 80 nm. It confirmed CdTe QDs were well conjugated with amino-modified Fe_3O_4 nanoparticles.

3.3.3 Magnetic characteristics

A vibrating sample magnetometer (VSM) was used to measure the magnetic properties of Fe_3O_4, amino-modified Fe_3O_4 and Fe_3O_4/CdTe nanoparticles. As shown in Fig. 4, the saturation magnetization of Fe_3O_4 nanoparticles was 71.37 emu/g (Fig. 4a), which was obviously higher than that (45.04 emu/g) of amino-modified Fe_3O_4 nanoparticles (Fig. 4b) due to the step-by-step fabrication. After amino-modified Fe_3O_4 nanoparticles were conbinded with non-magnetic CdTe QDs, the measured saturation magnetization of Fe_3O_4/CdTe composite particles was significantly decreased to 9.42 emu/g (Fig. 4c).

The solutions of Fe_3O_4/CdTe composite particles were placed under normal light (insert in Fig. 4.1) and 365 nm excitation (insert in Fig. 4.2). When a magnet was absent, the colors of the solutions (left side) under normal light and 365 nm excitation were yellow and fluorescent green, respectively, However, when the magnet was placed near the solutions, the magnetic fluorescence nanoparticles dispersed well in the solutions were attracted and concentrated near the magnetic field; both solutions had no colors (right side). All these results showed that Fe_3O_4/CdTe nanoparticles were successfully synthesized.

3.4 Characterization of PBA-functionalized Fe_3O_4/CdTe magnetic fluorescence nano probe

PBA was immobilized on the surface of Fe_3O_4/CdTe nanoparticles to recognize and detect SA. As shown in Fig. 2d of PBA-functionalized Fe_3O_4/CdTe, the IR absorption peak at 1359 cm^{-1} was assigned to the stretching vibration of B-O bond, which was also observed in PBA (Fig. 2e).The result indicated that PBA was successfully modified on Fe_3O_4/CdTe nanoparticles surface. As shown in Fig. 3d of DLS results, the average diameter of Fe_3O_4/CdTe nanoparticles was about 157.5nm, which was much bigger than that of TEM results. The reason was that the value under the condition of DLS represented the diameter of aqueous Fe_3O_4/CdTe nanoparticles , not dried nanoparticles. After modified with PBA, the average diameter of Fe_3O_4/CdTe nanoparticles was increased to 215.2nm (Fig. 3e). The result confirmed the successful conjugation between PBA and Fe_3O_4/CdTe nanoparticles. Fig. 5a, 5b and 5c showed the UV absorption and fluorescence emission spectra of CdTe QDs, Fe_3O_4/CdTe nanoparticles and PBA-functionalized Fe_3O_4/CdTe nano probe, respectively. As shown in Fig. 5b, the absorption spectrum of Fe_3O_4/CdTe nanoparticles was quite broad and shifed toward longer wavelength compared with that of CdTe QDs. Similarly, the red shift was observed in the fluorescence emission spectra of Fe_3O_4/CdTe nanoparticles. Compared with pure CdTe QDs, the fluorescence intensity of Fe_3O_4/CdTe was obviously decreased due to the magnetism of Fe_3O_4/CdTe. These phenomena indicated that the interaction between magnetic nanoparticles and CdTe QDs were taken place. After introducing PBA on the surface of Fe_3O_4/CdTe nanoparticles, the spectra properties had no obvious change due to PBA having little influence on the surface structure of CdTe QDs.

The agarose gel electrophoresis result showed that PBA-functionalized Fe_3O_4/CdTe nano probe moved slower than the pure Fe_3O_4/CdTe nanoparticles (inset in Fig. 5). It also indicated that PBA was successfully modified on the surface of Fe_3O_4/CdTe nanoparticles.

3.5 Selectivity and stability

The selectivity of PBA-functionalized Fe_3O_4/CdTe magnetic fluorescence nano probe for SA recognition was investigated by comparing SA alone with mixed solution of SA and other interferent. As shown in Fig. 6, the fluorescence intensity kept almost no changed when the mixed samples were added into the solution of the PBA-functionalized Fe_3O_4/CdTe nano probe, compared with that of SA alone. This result showed that PBA-functionalized Fe_3O_4/CdTe nano probe could selectively recognize SA. In addition, the stability of the functional nano probe was also evaluated. In Fig. 7, the fluorescence intensity of the as-prepared nano probe did

not change obviously within 12 h. It indicated that the as-prepared nano probe had relatively good stability, suggesting its practical utility.

3.6 Analytical performance of PBA-functionalized Fe_3O_4/CdTe nano probe

Fig. 8 showed the fluorescence emission spectra of PBA-functionalized Fe_3O_4/CdTe magnetic fluorescence nano probe added with different concentrations of SA. As expected, the fluorescence intensity decreased obviously with the increasing concentrations of SA. The decreasing fluorescence intensity was well linear with SA concentrations in the range of 50 μg/ml-1.50 mg/ml, and the liner equation is $(F_0\text{-}F)F_0=0.5617C+0.0020$ with R^2 of 0.9935 (Where, F_0 and F are the fluorescence intensities of PBA-functionalized Fe_3O_4/CdTe nano probe in the absence and presence of SA, respectively, C is the concentration of SA). The limit of detection of 16 μg/ml was obtained based on 3σ/k (Where, σ is the standard deviation of blank measurements (n=10), and k is the slope of calibration graph). As shown in Table 1, the intra-day relative standard deviations (RSDs) and the inter-day RSDs of this method were all less than 11.97%. These results suggested that the method exhibited a relatively broader linear range and had good precision.

3.7 Analytical application in real sample

To investigate the potential application of the proposed method, the PBA-functionalized Fe_3O_4/CdTe magnetic fluorescence nano probe was applied to the detection of SA in infant formula. The experiment results are shown in Table 2. According to the reference reported, addition levels of SA in infant formula are in the range of 0.8-1.2 mg/g.[28] The result of our detection was 0.82 mg/g, which coincided with the reference. Moreover, standard addition method was employed to verify the accuracy of the built method. As can be seen, the recoveries of the spiked SA at three different levels in the infant formula samples were from 85.45-92.98% with RSDs less than 8.35%. All the recoveries and RSDs of this method meet the requirements of trace sample analysis. It indicated that the PBA-functionalized Fe_3O_4/CdTe magnetic fluorescence nano probe can be used to monitor SA added in infant formula.

Different methods of SA detection are compared in Table S1. From the table we can see that the HPLC and fluorescence method have relatively lower LOD. However, the operation of HPLC method needs professional techniques and the fluorescence method in table S1 also needs expensive reagent such as enzyme, which also makes the protein-QDs not very stable. Although the sensitivity of our method was lower than some of the reported methods[13, 29], it is enough for the present probe to detect SA in infant formula, and it is more simple ,rapid and low-costing.

Conclusions

In this study, we established a facile method to determine SA using magnetic fluorescence nanoparticles and PBA-SA recognition system. Compared with the reported methods of SA detection, the method built has some advantages: (1) The synthesis of PBA-functionalized Fe_3O_4/CdTe magnetic fluorescence nano probe is facile, low-costing and rapid. (2) This fluorescence nano probe has high selectivity based on PBA-SA recognition system. (3) The conjugate of fluorescence nano probe and SA is easy to be separated from the sample matrix due to the magnetism of the nanoparticles. (4) The PBA-functionalized Fe_3O_4/CdTe magnetic fluorescence nano probe has high stability. So, the present probe has potential application in food quality control.

Acknowledgments

This work was financially supported by the National Natural Science Foundation of China (No. 81173016), Natural Science Foundation of Jiangsu Education Committee (No. 12KJB350003), and Technology Development Foundation of Nanjing Medical University (No. 2013NJMU023, 2013NJMU024).

References

1 E. Villar and I. M. Barroso, *Glycoconj. J.*, 2006, 23, 5-17.
2 B. L. G. Morgan and M. Winick , *J. Nutr.*, 1980, 110, 416-24.
3 Y. Massamiri, G. Durand, A. Richard, J. Féger and J. Agneray, *Anal. Biochem.*, 1979, 97 (2): 346-351.
4 P. Molor-Erdence, K. Okajima, H. Isobe, M. Uchiba, N. Harada, H. Okabe , *Am. J. Physiol. Heart Circ. Physiol.*,2005,288(3): H1265-H1271.
5 E. E. Brich, S. Garfield, D. R. Hoffman, R. Uavy and D. G. Brich, *Dev. Med. Child Neurol.*, 2000, 42, 174-181.
6 A. Tebani, D. Schlemmer, A. Imbard, O. Rigal and D. Porquet, *J. Chromatogr. B*, 2011, 879, 3694-3699.
7 K. Matsuno and S. Suzuki, *Anal. Biochem.*, 2008, 375, 53-59.
8 S. A. M. Marzouk, S. S. Ashraf and K. A. Tayyari, *Anal. Chem.*, 2007, 79, 1668-1674.
9 X. R. Zhang, M. S. Liu, H. X. Liu and S. H. Zhang, *Biosens. Bioelectron.*, 2014, 56, 307-312.
10 L. I. Liu, Q. Ma, Z. P. Liu, and X. G. Su, *Biosens. Bioelectron.*, 2015, 63, 519-524.
11 Z. P. Liu, L. I. Liu, M. H. Sun and X. G. Su, *Biosens. Bioelectron.*, 2015, 65, 145-151.
12 L. L. Huang, Y. J. Jin, D. X. Zhao, C. Yu, J. Hao and H. Y. Xie, *Anal. Bioanal. Chem.*, 2014, 406 (11): 2687-2693.
13 Y. L. Zhou, H. Dong, L. T. Liu, J. Liu and M. T. Xu, *Biosens. Bioelectron.*, 2014, 60, 231-236.
14 A. P. Liu, S. Peng, J. Chow Soo, M. Kuang, P. Chen and H. W. Duan, *Anal. Chem.*, 2011, 83,1124-1130.
15 E. Han, L. Ding and H.X. Ju, *Anal. Chem.*, 2011, 83, 7006-7012.
16 H. Otsuka, E. Uchimura, H. Koshino, T. Okano and K. Kataoka, *J. Am. Chem. Soc.*, 2003, 125 (12): 3493-3502.
17 A. Matsumoto, N. Sato, K. Kataoka and Y. Miyahara, *J. Am. Chem. Soc.*, 2009, 131, 12022-12023.
18 J. Xie, C. Xu, N. Koher, Y. Hou and S. Sun, *Adv. Mater.*, 2007, 19 (20): 3163.
19 P. Sun, H. Y. Zhang, C. Liu, J. Fang, M. Wang, J. Chen, J. P. Zhang, C. B. Mao and S. K. Xu, *Langmuir*, 2010, 26(2): 1278-1284.
20 J. M. Zhang, S. R. Zhai, S. Li, Z. Y. Xiao, Y. Song, Q. D. An and G. Tian, *Chem. Eng. J.*, 2013, 215-216, 461-471.
21 F. D. Wei, X. L. Lu, Y. Z. Wu, Z. Cai, L. Liu, P, Zhou and Q. Hu, *Chem. Eng. J.*, 2013, 226, 416-422.
22 J. M. Shen, W. J. Tang, X. L. Zhang, T. Chen, H. X. Zhang, *Carbohydr. Polym.*, 2012, 88, 239-249.
23 F. D. Wei, Y. Lin, Y. Z. Wu, X. Su, L. P. Liu, P. Zhou and Q. Hu, *Anal. Methods*, 2014, 6, 482-489.
24 S. Y. Liu, F. P. Shi, X. J. Zhao, L. Chen and X. G. Su, *Biosens. Bioelectron.*, 2013, 47, 379-384.
25 M. Y. Gao, S. Kirstein, H. Mohwald, A. L. Rogach, A. Kornowski, A. Eychmuller and H. Weller, *J. Phys. Chem. B*, 1998, 102, 8360-8369.
26 F. D. Wei, X. L. Lu, Y. Z. Wu, Z. Cai, L.P. Liu, P. Zhou and Q. Hu, *Chem.Eng. J.*, 2013, 226, 416-422.
27 Y. F. Liu and J. S. Yu, *J. Colloid Interf. Sci.*, 2009, 33, 690-698.
28 M. J. Martin, E. Vazquez and R. Rueda, *Anal. Bioanal. Chem.*, 2007, 387, 2943-2949.
29 D. H. Li, *Food Sci. Biotechnol.*, 2012, 21(5): 1317-1320.

Figure captions

Scheme 1. Schematic illustration of synthesis of PBA-functionalized Fe_3O_4/CdTe nano probe and its working principle for SA detection.

Fig. 1. Influence of (a) different ratios of MPA-capped QD to amino-modified Fe_3O_4 and (b) pH value on fluorescence intensity of PBA-functionalized Fe_3O_4/CdTe nano probe.

Fig. 2. FT-IR spectra of (a) Fe_3O_4, (b) amino-modified Fe_3O_4, (c) Fe_3O_4/CdTe, (d) PBA-functionalized Fe_3O_4/CdTe nano probe, and (e) PBA.

Fig. 3. TEM images of (a) Fe_3O_4, (b) amino-modified Fe_3O_4, (c) Fe_3O_4/CdTe; DLS results of (d) Fe_3O_4/CdTe and (e) PBA-functionalized Fe_3O_4/CdTe nano probe.

Fig. 4. VSM magnetization curves of (a) Fe_3O_4 nanoparticles, (b) amino-modified Fe_3O_4 nanoparticles, (c) Fe_3O_4/CdTe nanoparticles. The inset shows photographic images of aqueous solutions of Fe_3O_4/CdTe nanoparticles without a magnetic field (left) and with a magnetic field (right) under 365 nm excitation (1) and normal light (2).

Fig. 5. UV-vis absorption and fluorescence emission spectra of (a) CdTe QDs, (b) Fe_3O_4/CdTe nanoparticles, (c) PBA-functionalized Fe_3O_4/CdTe nano probe. The inset shows agarose gel electrophoresis of (b) Fe_3O_4/CdTe nanoparticles, (c) PBA-functionalized Fe_3O_4/CdTe nano probe.

Fig. 6. Responses of PBA-functionalized Fe_3O_4/CdTe nano probe to SA alone and mixed solution of SA and other interferent: SA (2 mM), Na^+ (2mM), K^+ (2mM), Mg^{2+} (0.3mM), Ca^{2+} (0.2mM), Fe^{3+} (0.02mM), Zn^{2+} (0.01mM), Cu^{2+} (1μM), Hg^{2+} (10nM), Pb^{2+} (100nM), Mn^{2+}(1μM), Vc (0.1mM), BSA (7.5mg/l), DA (0.8 mM), Glu (2 mM), Gal (2 mM), Man (2 mM), Fru (0.8 mM).

Fig. 7. Stability of PBA-functionalized Fe_3O_4/CdTe nano probe.

Fig. 8. Fluorescence spectra of PBA-functionalized Fe_3O_4/CdTe nano probe in the presence of various concentrations of SA (from a to j: 0, 0.05, 0.10, 0.20, 0.40, 0.60, 0.80, 1.00, 1.20 and 1.50 mg/ml). The insert shows the calibration curve of the SA detection.

Table 1 Precisions of SA determination by PBA-functionalized Fe_3O_4/CdTe nano probe (n=5)

Concentration of SA (mg/ml)	intra-day (mg/ml)	RSD (%)	inter-day (mg/ml)	RSD (%)
0.10	0.10	11.76	0.10	11.97
	0.08		0.12	
	0.10		0.12	
0.60	0.57	1.74	0.57	6.21
	0.57		0.63	
	0.55		0.56	
1.20	1.26	0.52	1.26	1.59
	1.26		1.24	
	1.24		1.22	

Table 2 Determination of SA in infant formula (n=5)

samples	Spiked (mg/g)	Found (mg/g)	Recovery (%)	RSD (%)
1	0	0.82	-	4.26
2	4.00	4.24	85.45	8.35
3	8.00	7.74	86.51	4.49
4	12.00	11.98	92.98	3.54

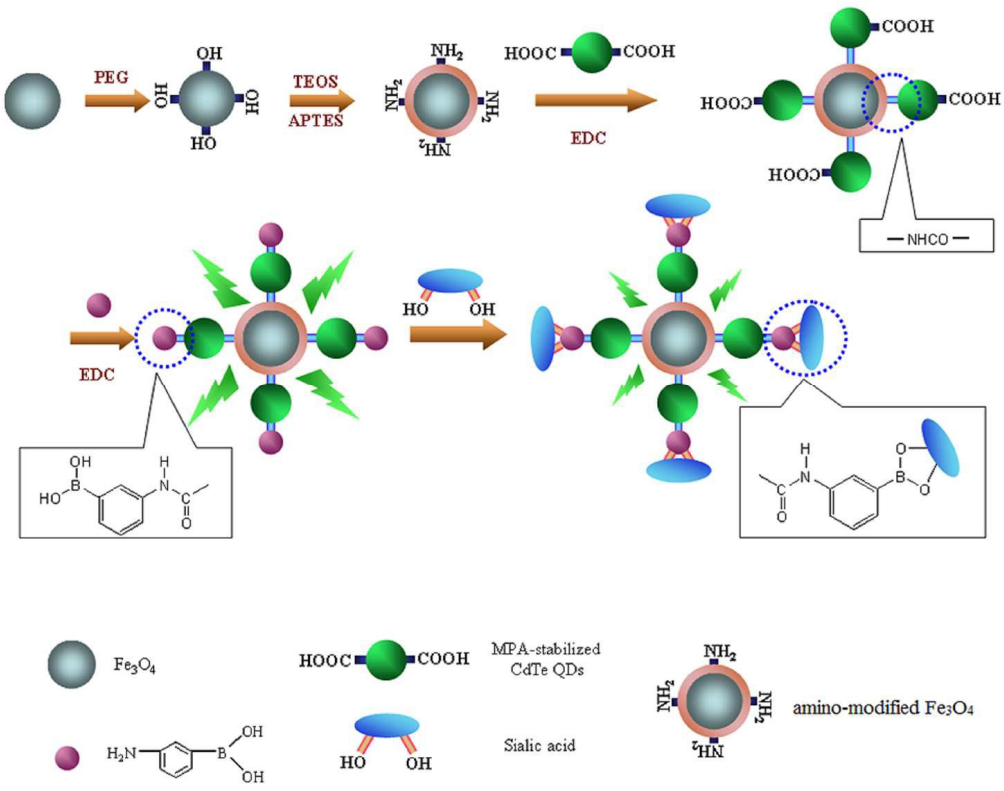

Scheme 1

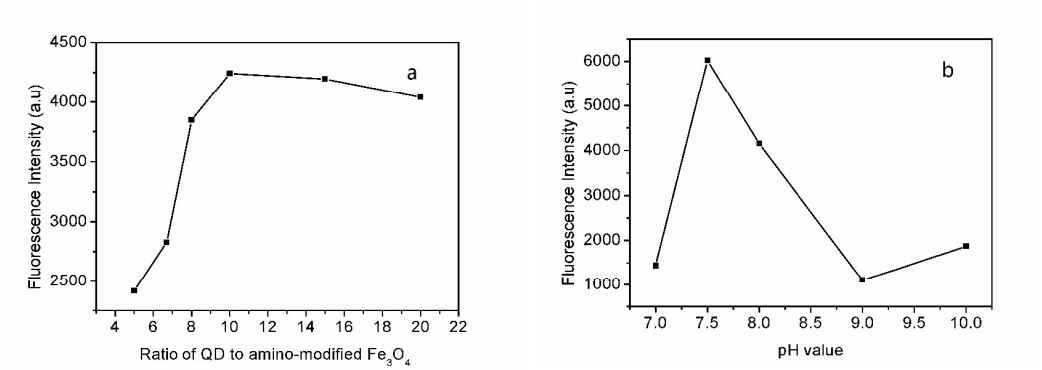

Fig. 1

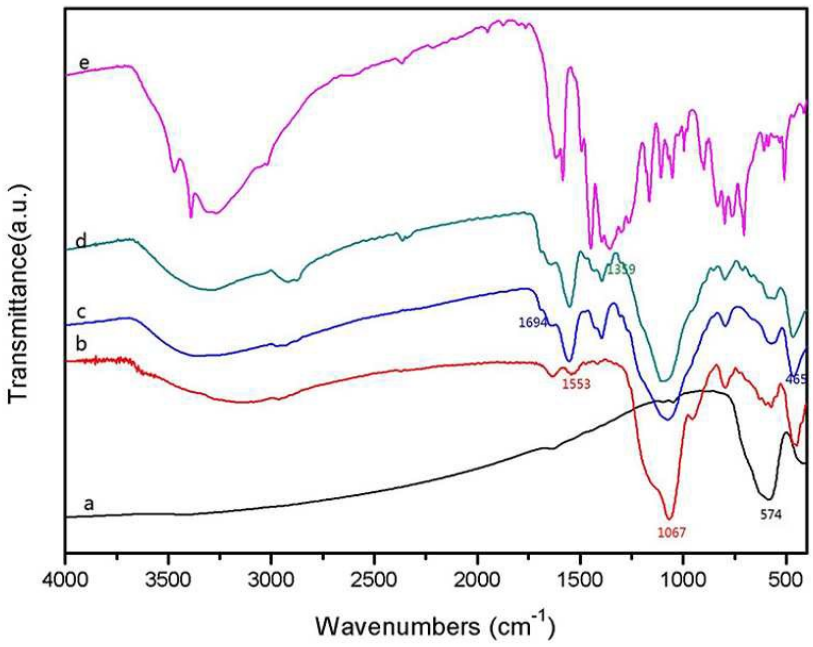

Fig. 2

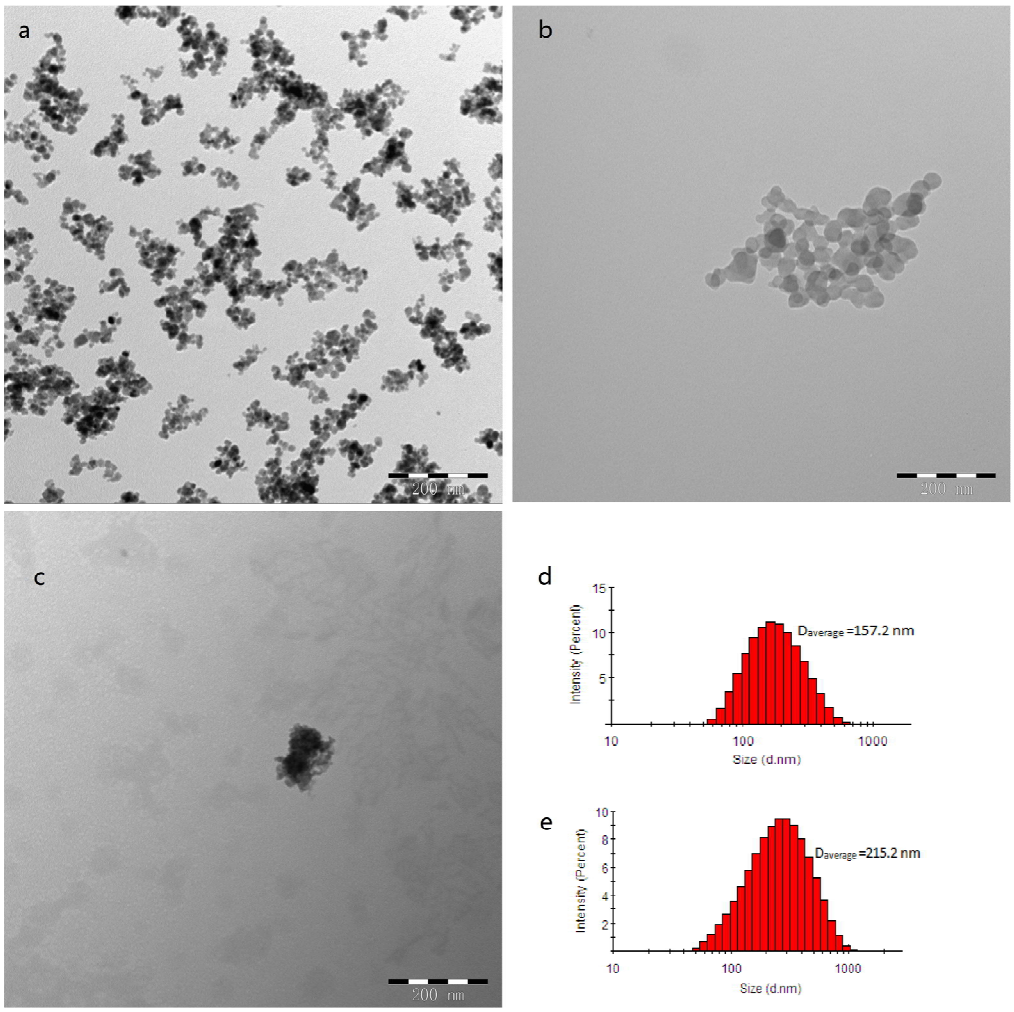

Fig. 3

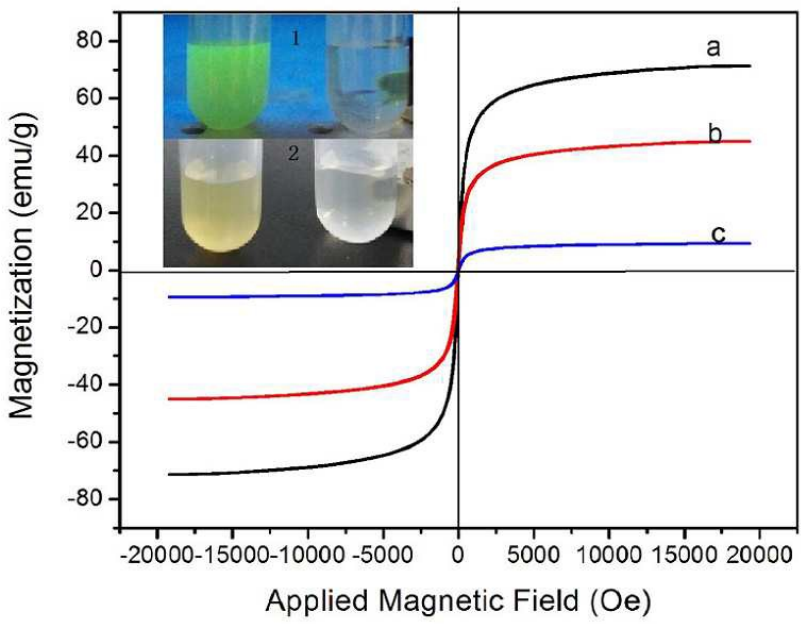

Fig. 4

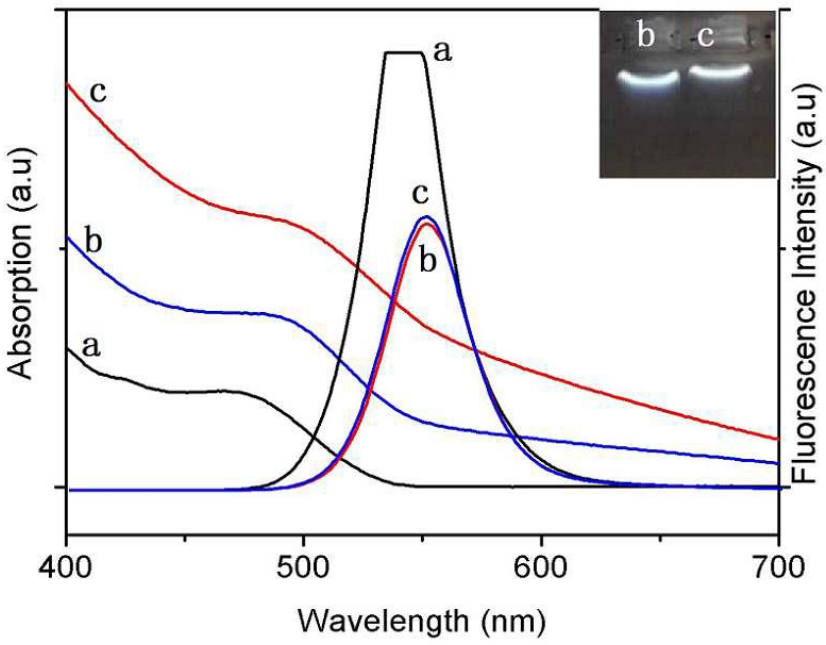

Fig. 5

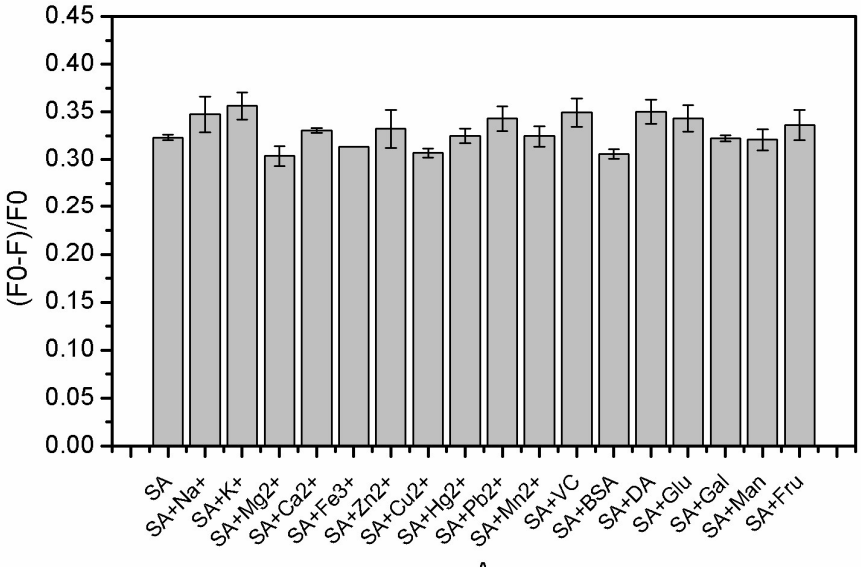

Fig. 6

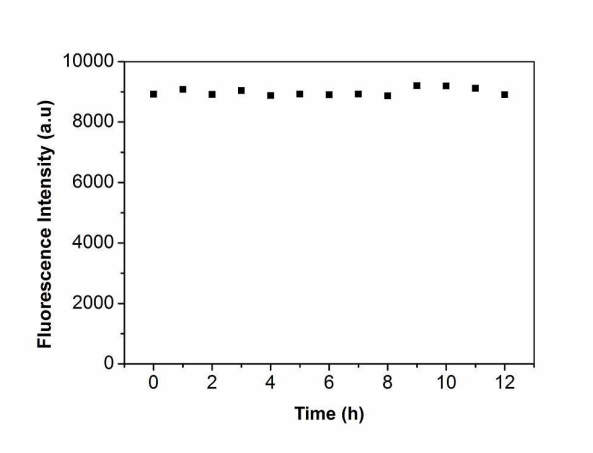

Fig. 7

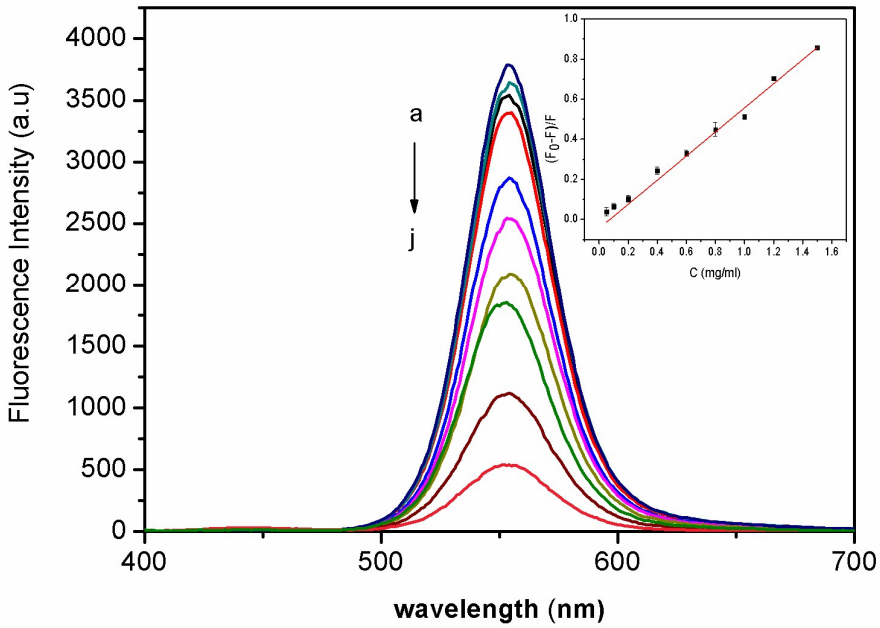

Fig. 8